

[M]acro-
olecular
Rapid Communications

Supporting Information

for *Macromol. Rapid Commun.*, DOI 10.1002/marc.202200554

Transparent and Self-Healing Elastomers for Reconfigurable 3D Materials

Tiwa Yimyai, Abdon Pena-Francesch and Daniel Crespy**

Supporting Information

Transparent and self-healing elastomers for reconfigurable 3D materials

Tiwa Yimyai, Abdon Pena-Francesch,* and Daniel Crespy*

* Corresponding Author. *E-mail address:* daniel.crespy@vistec.ac.th

Table of contents

Figure S1: ¹H-NMR spectra of self-healing polymer (PU-SH) and non-self-healing polymer (PU)

Figure S2: Storage and loss moduli of PU as a function of frequency sweep at 10–90 °C

Figure S3: Formation of 3D objects by folding and assembly

Figure S4: Storage and loss moduli of PU-SH as a function of frequency and strain sweep

Figure S5: Ultraviolet-visible (UV-vis) transmittance spectra of materials

Figure S6: Fabrication of a self-healing plastic cuvette

Figure S7: UV-vis light scattering spectra (T_4) of PU-SH and PU

Figure S8: UV-vis absorption spectra and calibration curves of methylene blue using quartz cuvette

Figure S9: UV-vis absorption spectra of methyl orange using quartz and polystyrene cuvettes

Figure S10: 3D shape changes of a self-healing polymer cylinder

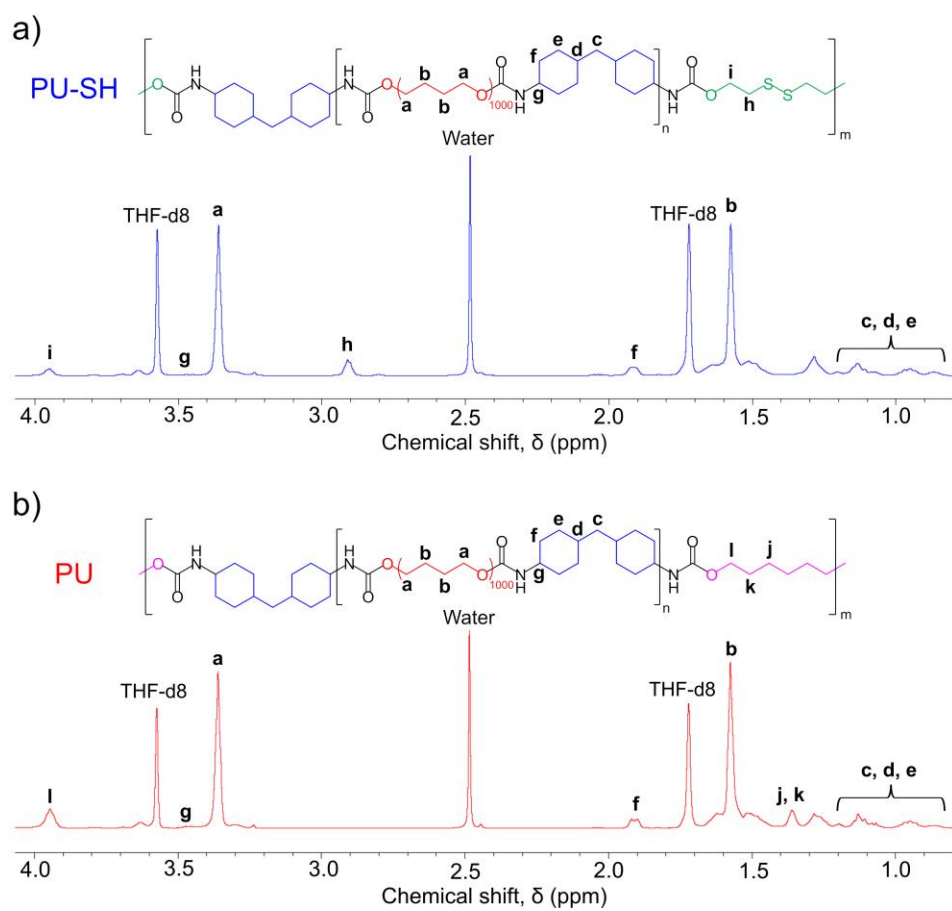


Figure S1. ^1H nuclear magnetic resonance (^1H -NMR) spectra of a) self-healing polymer (PU-SH) and b) non-self-healing polymer (PU) in THF-d8.

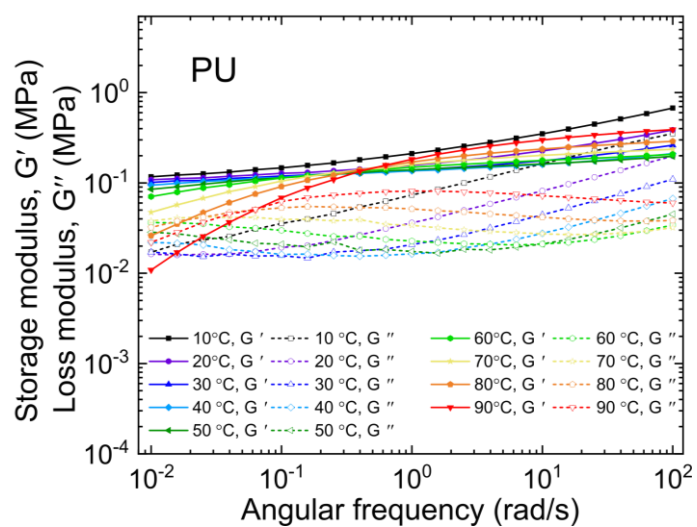


Figure S2. Storage modulus (G') and loss modulus (G'') as a functions of frequency sweep at different sweeping temperature for non-self-healing polymer (PU).

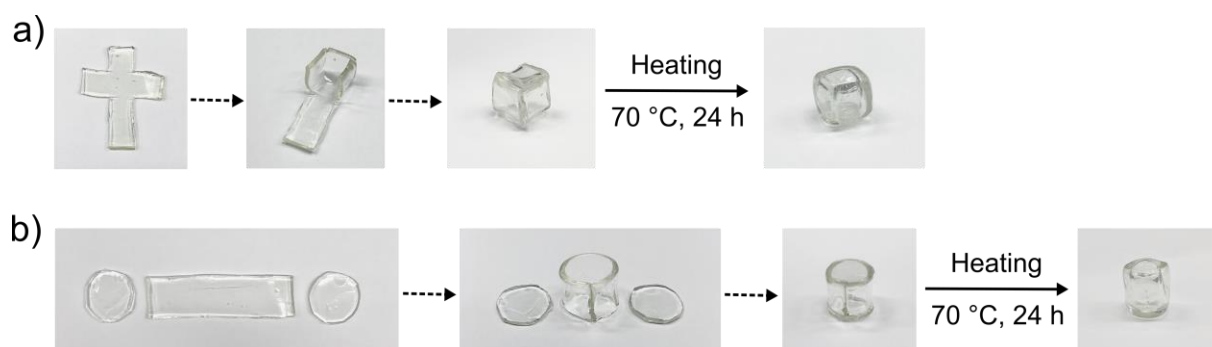


Figure S3. Photographs showing the formation of 3D objects by a) folding and b) assembling 2D polymer sheets to obtain a hollow cube and a hollow cylinder, respectively.

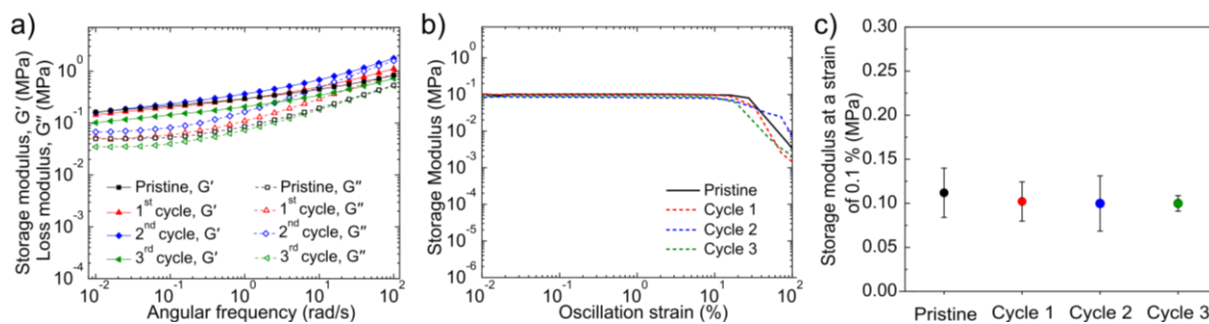


Figure S4. a) Storage modulus (G') and loss modulus (G'') as a functions of frequency sweep at 25 °C for PU-SH before and after being subjected to a cycle of shape programming (heating at 70 °C for 24 h, and then cooling down to 25 °C). b) Representative curves of storage modulus as a function of oscillation strain (%) under a frequency of 0.1 Hz for circular polymer sheets before and after three cycles of deformation-recovery by heating. c) Storage moduli (G') at a strain of 0.1% of self-healing polymer sheets before after several cycles of deformation-recovery by heating. The moduli were extracted from linear viscoelastic region of dynamic mechanical analysis in shear mode under a frequency of 0.1 Hz and a dynamic strain sweep of 0.01 to 100% at 25 °C.

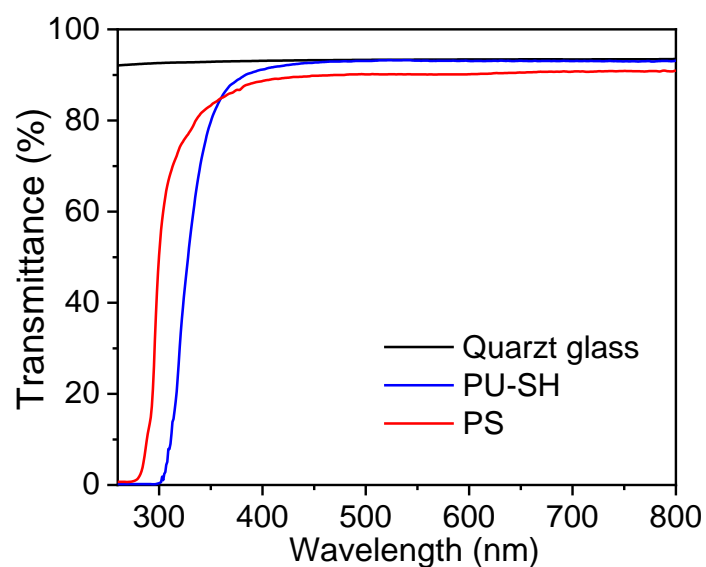


Figure S5. Ultraviolet-visible (UV-vis) transmittance spectra of a quartz glass substrate (thickness = 1.0 mm), a self-healing polymer sheet (thickness = 0.78 ± 0.02 mm), and a polystyrene substrate (thickness = 1.0 mm).

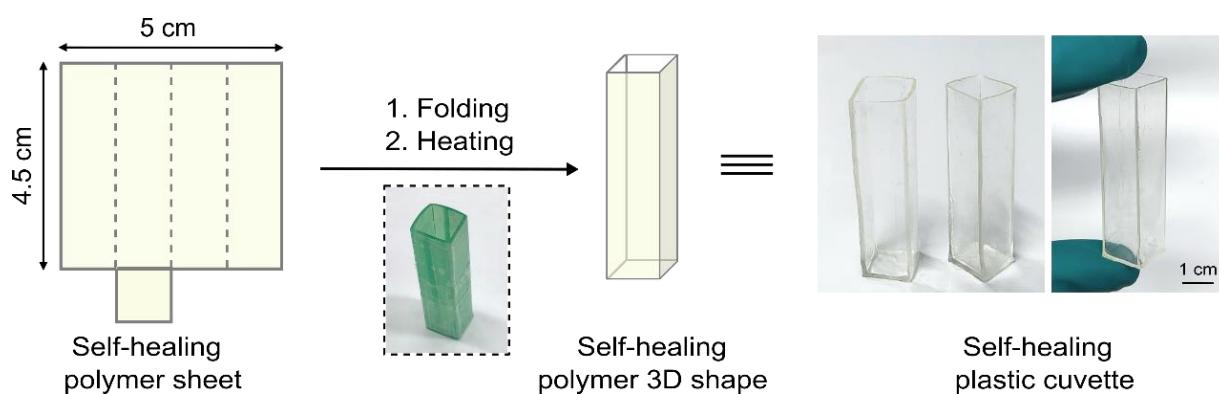


Figure S6. Fabrication of a self-healing plastic cuvette by folding a planar polymer sheet into a hollow rectangular prim.

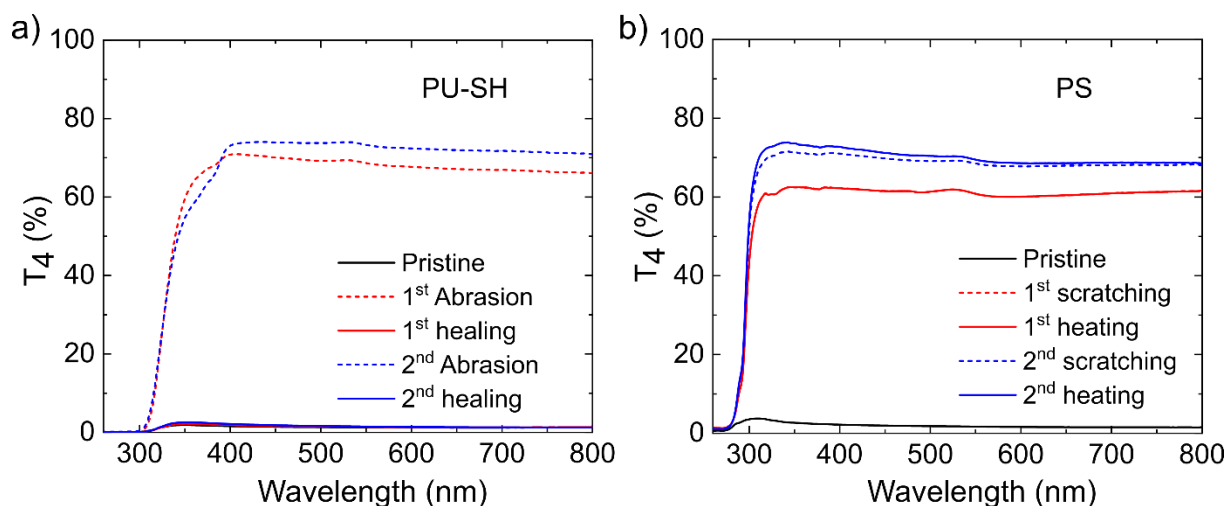


Figure S7. Ultraviolet–visible (UV-vis) spectra for light scattering of instrument and samples (T_4) of a) a self-healing polymer (PU-SH) substrate (thickness = 0.78 ± 0.02 mm) and b) a polystyrene (PS) substrate (thickness = 1.0 mm).

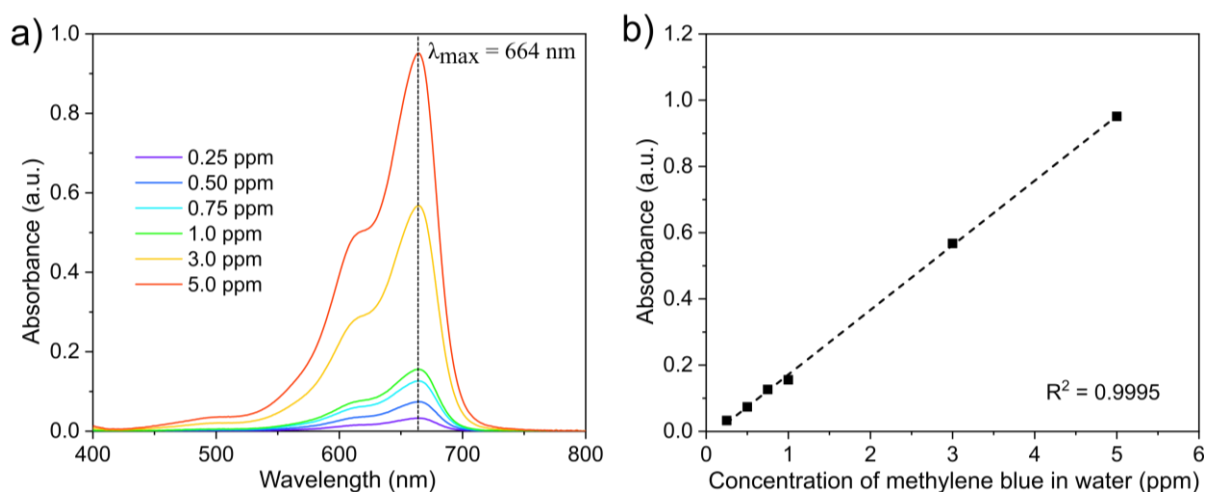


Figure S8. a) Ultraviolet–visible (UV-vis) absorption spectra of methylene blue aqueous solution with various concentrations, which were measured in a quartz cuvette. b) Relationships between UV-vis absorbance at $\lambda_{\max} = 664$ nm and concentrations of methylene blue aqueous solutions.

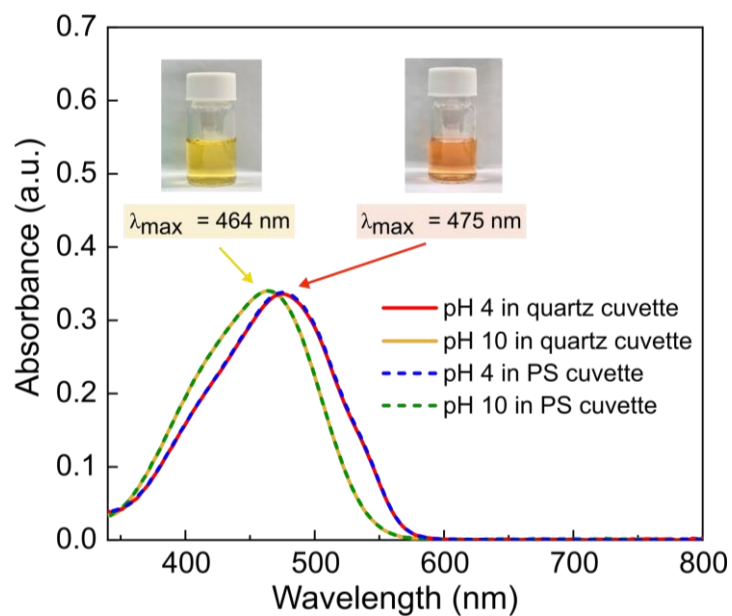


Figure S9. UV-vis absorption spectra of methyl orange aqueous solutions at pH 4 and 10, which were measured using quartz and polystyrene (PS) cuvettes.

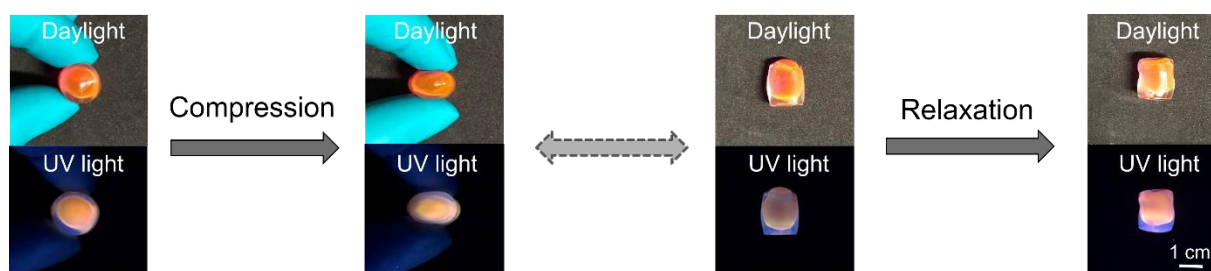


Figure S10. 3D shape changes of a self-healing polymer cylinder containing an aqueous solution of Rhodamine B by mechanical compression and relaxation at 25 °C.